

Properties of an inclined standpipe for feeding solids into a bubbling fluidized-bed

Yoo Sube Won*, Gyoung-Woo Lee*, Daewook Kim*, A-Reum Jeong*,
Jeong-Hoo Choi^{*,†}, Sung-Ho Jo^{**}, and Chang-Keun Yi^{**,†}

*Department of Chemical Engineering, Konkuk University, 120 Neungdong-ro, Gwangjin-gu, Seoul 05029, Korea

**Korea Institute of Energy Research, 152 Gajeong-ro, Yuseong-gu, Daejeon 34129, Korea

(Received 10 February 2017 • accepted 24 May 2017)

Abstract—Flow properties of solids in an inclined standpipe were investigated while the solid particle was fed to the bottom of a bubbling fluidized bed (diameter 0.1 m, 1.34 m tall) via the standpipe and discharged out of the bed through the overflow exit. A group of K-based CO₂ adsorbent particles was used as solids. The pressure drop of the fluidized bed, the height of solids bed in the standpipe, and flow rate of gas bypassing the fluidized bed through the standpipe were measured at room temperature and pressure as varying the fluidizing gas velocity, solids flow rate, and height of the overflow exit of fluidized solids. The pressure drop of the fluidized bed, the height of the solids bed in the standpipe, and the ratio of gas bypassing through the standpipe to the total gas in flow rate decreased with increasing the fluidizing gas velocity. Both the pressure drop of the fluidized bed and the height of the solids bed in the standpipe increased a little with the solids feed rate. The effect of the solids feed rate on the flow rate of gas bypassing through the standpipe could be ignored. The pressure drop of the fluidized bed and the height of the solids bed in the standpipe increased as the height of the overflow exit for solids increased in the fluidized bed. However, the effect of the height of the overflow exit on the flow rate of gas bypassing through the standpipe was negligible. Correlations on the pressure drop of the fluidized bed, the height of the solids bed in the standpipe, and the flow rate of gas bypassing through the standpipe were proposed successfully.

Keywords: Standpipe, Dipleg, Cyclone, Bubbling Bed, Fluidized Bed

INTRODUCTION

The cyclone is often used for separating solids and fluid, respectively, out of the mixture of fluid and solids. Solids separated from gas in the gas cyclone are lowered along the dipleg. If the dipleg is connected to an isolated container, there is little gas flow upward in the dipleg. In other case that the solids are transported to the next process through the dipleg, which gas flow to the downstream process or from the downstream process must be suppressed completely in order to maintain a high collection efficiency of the cyclone. Although either the mechanical or non-mechanical valve is often used for this purpose, any one cannot block the flow of gas at all [1].

The atmospheric circulating fluidized bed (CFB) process that uses K₂CO₃ adsorbent for capturing CO₂ from the combustion gas is composed of the adsorption tower (riser), the cyclone, the regeneration column (bubbling bed) [2,3]. Combustion gas containing CO₂ is introduced into the riser as fluidizing gas. The adsorbent particle is typically stored in the bubbling bed and is fed by gravity to the bottom of the riser according to the flow rate at the given K₂CO₃/CO₂ molar ratio. Particles adsorbing CO₂ and moisture in the riser are transported by the combustion gas out of the riser, separated from the gas in the cyclone and falling by gravity along the dipleg into the bubbling bed. In the bubbling bed, adsorbent

solids are regenerated releasing water and CO₂. Then the solids complete a turn of the external circulation loop [2,3]. The cyclone of the riser and the freeboard of the bubbling bed in the loop are maintained at the working pressure substantially equal.

Here are some considerations on the dipleg of the riser cyclone of the CO₂ capture process. 1) To obtain a high collection efficiency of the cyclone, the influx of gas from the regenerator to the cyclone should be suppressed. It also needs to prevent the loss of captured CO₂. 2) Contrarily, the concentration of the captured CO₂ gas must not be diluted by the cyclone gas being introduced into the regeneration column. 3) Therefore, unlike most of the standpipe [1,4-11] the dipleg should avoid aeration from the outside. If it is needed, the aeration using the captured CO₂ gas should be made into the regenerator.

As a result, the hybrid dipleg [1,4,7,9], a combination of the vertical and inclined tube, is used without any valve and aeration as a dipleg that satisfies the above considerations. That is inserted through the outer wall of the regeneration column and the solids bed moving downward suppresses the reverse flow of gas within the dipleg. The concerns in this dipleg are the rate of backflow gas and the height of the solids bed, and the influencing variables are the solids flow rate, the level of the solids inlet, and the fluidizing velocity within the regeneration column.

Youn and Choi [12] tested a similar standpipe located between two-stage bubbling fluidized beds. The standpipe was connected between the surface of the upper bed and the bottom of the lower bed. The solids were continuously fed to the bed and discharged out of the bed through the standpipe by overflow. Solids were first

[†]To whom correspondence should be addressed.

E-mail: choijhoo@konkuk.ac.kr, ckyi@kier.re.kr

Copyright by The Korean Institute of Chemical Engineers.

fed just below the surface level of the upper bed, but the solids overflowing out of upper bed were fed to the bottom of the lower bed via the first standpipe. The solids out of the lower bed were sent to the storage hopper via the second standpipe. The exit gas of the lower fluidized bed was fed to the upper bed as the fluidizing gas and there was no aeration into the standpipe. They examined the conditions in which the first standpipe was able to work safely. They investigated the fluidizing velocity of the lower bed when within the standpipe the gas punched the solids bed by pushing them back. However, they did not measure the gas flow rate and the height of the solids bed within the standpipe at the velocity. Other similar studies were rare.

The purpose of this study was to investigate the flow properties of solids in an inclined standpipe while the solid particle was fed to the bottom of a bubbling fluidized bed via the standpipe and discharged out of the bed by overflow. This process was designed to simulate the flow characteristics within the dipleg placed under the cyclone of the CFB riser of the CO₂ capture process mentioned above. A group of K-based CO₂ adsorbent particles was used as solids. Varying the fluidizing gas velocity, solids flow rate, and height of the overflow exit of fluidized solids, we considered the height of solids bed and gas flow rate in the standpipe and the pressure drop of the fluidized bed at room temperature and pressure.

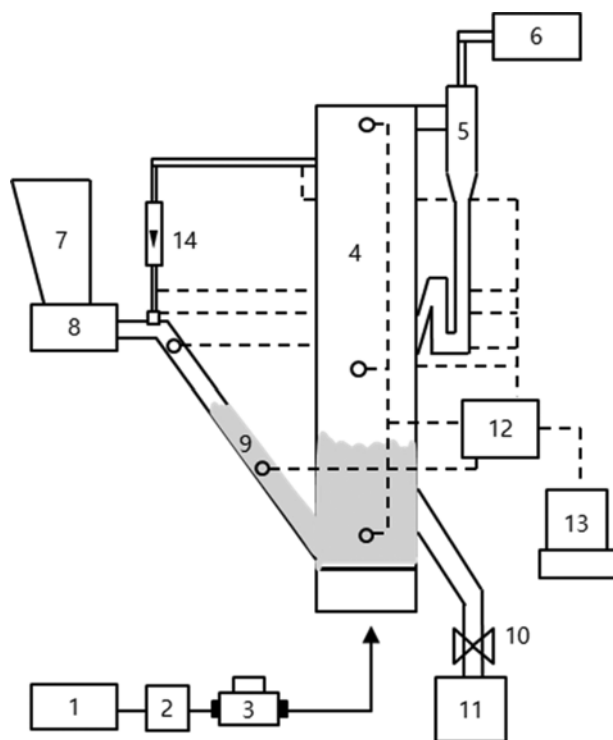


Fig. 1. Flow diagram of the experimental setup.

- | | |
|------------------------------|---|
| 1. Compressor | 9. Solids-feeding standpipe |
| 2. Filter | 10. Ball valve |
| 3. Mass flowmeter controller | 11. Drain hopper |
| 4. Bubbling fluidized bed | 12. Data logging system with pressure transducers |
| 5. Cyclone and loopseal | 13. Personal computer |
| 6. Bagfilter | 14. Gas-bypassing line with a rotameter |
| 7. Feed hopper | |
| 8. Screw conveyor | |

EXPERIMENT

Fig. 1 shows the flow diagram of the laboratory-scale bubbling fluidized-bed process used in this experiment. The process consisted of an air supply system, a feed hopper, a screw conveyor, a solids-feeding standpipe (50 mm-i.d., 60 degree-angled from the horizontal plane), a bubbling fluidized-bed (Plexi-glass, 0.1 m-i.d., 1.34 m tall), a cyclone, a loopseal, a bagfilter and a drain hopper.

The feed hopper was charged with solids and sealed from the outside. The screw conveyor drew solids out of the feed hopper and controlled the flow rate by the rotating speed of it. Solids descended along the standpipe by gravity and flew into the lower part of the fluidized bed (50 mm-height from the distributor level). A gas outlet leading through a rotameter to the freeboard top of the fluidized bed was installed at the top of the standpipe (1 m-height from the distributor level) for gas rising along the standpipe to return to the fluidized bed. The gas flow rate was measured by the rotameter. The returning gas line was to simulate the gas flow back through the dipleg of the riser cyclone in the CO₂ capture process.

Air was supplied by a compressor, passed through a pressure regulator, a filter and a mass flow meter controller, and was injected through the plenum and the perforated plate (orifice diameter: 1 mm; number of orifices: 35) as fluidizing gas into the fluidized bed at atmospheric temperature and pressure. The freeboard gas containing entrained solids flowed into the cyclone through the gas outlet at the top of the freeboard, and after being separated from the solids in the cyclone was discharged to the atmosphere through the bag filter. All of the separated solids were re-injected into the fluidized bed through the loopseal and the amount of solids discharged to the atmosphere with the gas was negligible. Solids in the fluidized bed were discharged through the overflow drain outlet and flew into the drain hopper by gravity. Solids outlets were installed at three different heights (0.25, 0.4, 0.55 m height from the distributor level) to vary the depth of the solids bed over the solids inlet. To measure the axial pressure distribution of the fluidized bed, pressure taps were installed at various heights (-0.05, 0.05, 0.19, 0.89, 1.29, 1.34 m height from the distributor level). The bed pressure drop was measured between 0.05 m and 1.34 m in height.

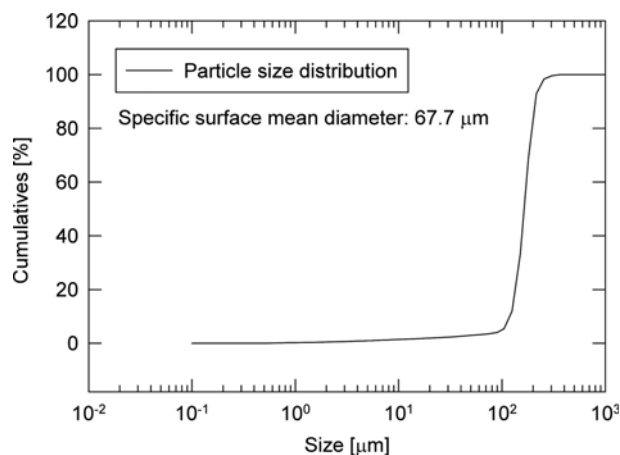


Fig. 2. Particle size distribution of particles.

Table 1. Ranges of experimental variables

Properties	Unit	Range
Fluidizing velocity	m/s	$3u_{mf}$ - $15u_{mf}$
Solids feed rate	g/s	1.89-8.25
Solids flux based on bed area	kg/m ² s	0.241-1.05
Solids flux based on standpipe area	kg/m ² s	0.963-4.20
Solids velocity based on standpipe area	m/s	0.000963-0.00420
Vertical solids velocity based on standpipe area	m/s	0.000834-0.00364
Height of overflow exit from distributor level	m	0.25, 0.4, 0.55

Maximum solids flux in CO₂ capture process: 1.85 kg/m²s (based on regenerator area), 105 kg/m²s (based on standpipe area)

The solid particles were K-based adsorbents (apparent density: 1,770 kg/m³, bulk density: 1,000 kg/m³, specific surface mean diameter ($=1/(\sum_i^N(x_i/d_{p,i}))$): 0.0677 mm, see Fig. 2 for size distribution) used in the CO₂ capture process [13]. The minimum fluidization velocity was measured 0.0125 m/s and the terminal velocity was calculated 0.75 m/s at the mean diameter [14]. The experimental method was as follows. Depending on the respective flow rates, the fluidizing gas was first introduced, followed by the solids. After filling the fluidized bed, solids overflowed out of the bed through the solids outlet. After reaching steady state, pressure drop across the fluidized bed, height of the solids bed within the solids-feeding standpipe, and the gas flow rate through the standpipe were measured as arithmetic mean values.

The fluidization velocity based on the total gas flow rate, the solids feed rate, and the height of the overflow exit for fluidized solids were considered as variables. Table 1 shows the range of each experimental variable. In the regenerator of the CO₂ capture process, the fluidization velocity was five- to ten-times the minimum fluidization velocity (u_{mf}), and the solids injection rate was about 1.85 kg/m²s based on the regenerator's cross-sectional area and about 105 kg/m²s based on the standpipe's cross-sectional area. The range of fluidization velocity was set considering the actual process velocity. However, because the apparatus of this experiment was small, the solids flux based on the sectional area of the fluidized bed was adjusted to be similar to the actual process value instead of the solids flux based on the sectional area of the standpipe.

RESULTS AND DISCUSSION

Effects of gas velocity and solids feed rate were investigated while the height of the overflow exit for fluidized solids was fixed at 0.55 m. Fig. 3(a) shows the change in the pressure drop across the fluidized bed with increasing gas velocity at various solids feed rates. The increase in gas velocity reduced the bed pressure drop. Because the bed pressure drop is proportional to the amount of solids, this means a reduction in the amount of solids in the bed. The solids are transported upwards by the wake of the bubble and discharged through the overflow exit by gravity. As the gas velocity increases, the volumetric flow rate of the bubbles increases. Because the volume of the bubble wake is proportional to the volume of bubble [15], the rate of solids transport increases with increasing gas velocity [16]. Therefore, the residence time and amount of solids in the bed decrease. Fig. 3(b) shows the change in the pressure

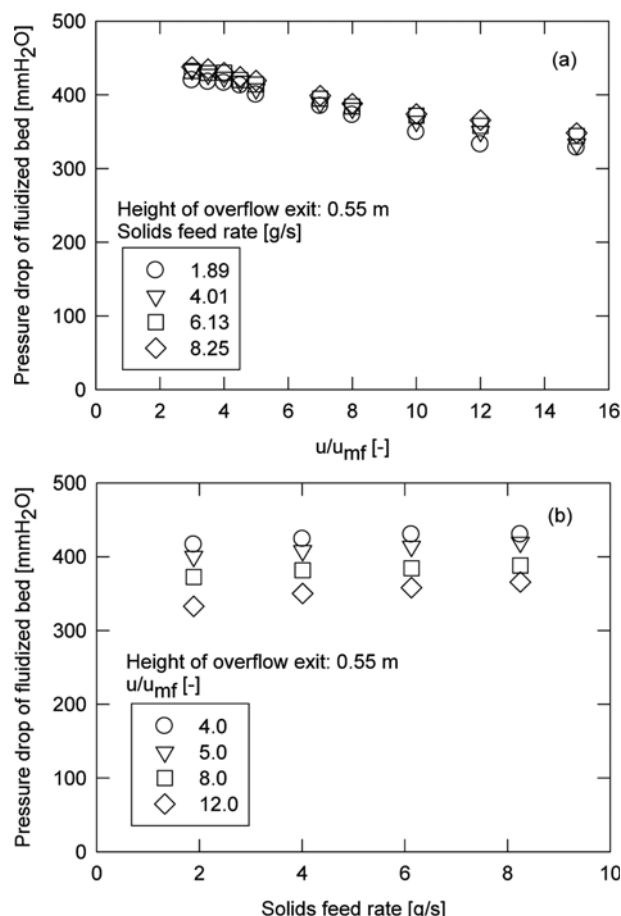


Fig. 3. Pressure drop across the fluidized bed (height of overflow exit for fluidized solids: 0.55 m): effects of (a) u/u_{mf} and (b) solids feed rate.

drop across the bed with increasing the solids feed rate at various gas velocities. As the solids feed rate increased, the pressure drop across the fluidized bed increased. When the gas velocity is constant, the solids transportation rate by bubbles is almost constant. Thus, as the solids feed rate increased, the residence time and amount of solids in the bed increased. The bed pressure drop was more influenced by the gas velocity than the solids feed rate.

Fig. 4(a) shows the change of height of the solids bed in the standpipe where the fed solids were moving down as the gas velocity in the fluidized bed increased at various solids feed rates. The

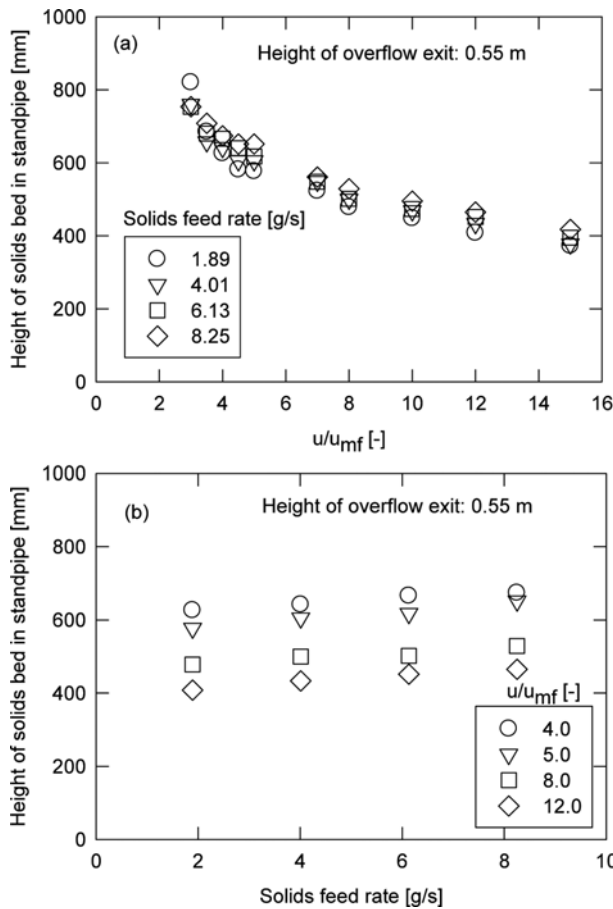


Fig. 4. Height of solids bed in the standpipe (height of overflow exit for fluidized solids: 0.55 m): effects of (a) u/u_{mf} and (b) solids feed rate.

solids in the standpipe were pushed into the fluidized bed by their own head, the height of solids bed. The height of solids bed in the standpipe decreased with increasing gas velocity. As shown in Fig. 3(a), the pressure drop across the fluidized bed decreased with increase in fluidizing velocity. The effect reduced the static pressure by the solids head at the height of the solids inlet in the fluidized bed. Thus, the counter-head that should be built in the standpipe for solids to get into the fluidized bed was reduced. In the standpipe, the descending velocity of the solids increased with decreasing the solids bed height. Fig. 4(b) shows the height of the solids bed in the standpipe with increasing the solids feed rate at various fluidizing gas velocities. The height of solids bed in the standpipe increased as the solids feed rate increased. According to Fig. 3(b), the pressure drop across the fluidized bed increased as the solids feed rate increased. The effect increased the static pressure by the solids head at the height of the solids inlet in the fluidized bed. It also increased the solids head that should be built in the standpipe for the solids to enter the fluidized bed. The solids-bed height in the standpipe was more influenced by the fluidizing velocity than the solids feed rate.

Bypassing the fluidized bed, part of the fluidizing gas flowed to the freeboard through the standpipe in which the solids moved down. Fig. 5(a) shows the flow rate of the gas bypassing the fluid-

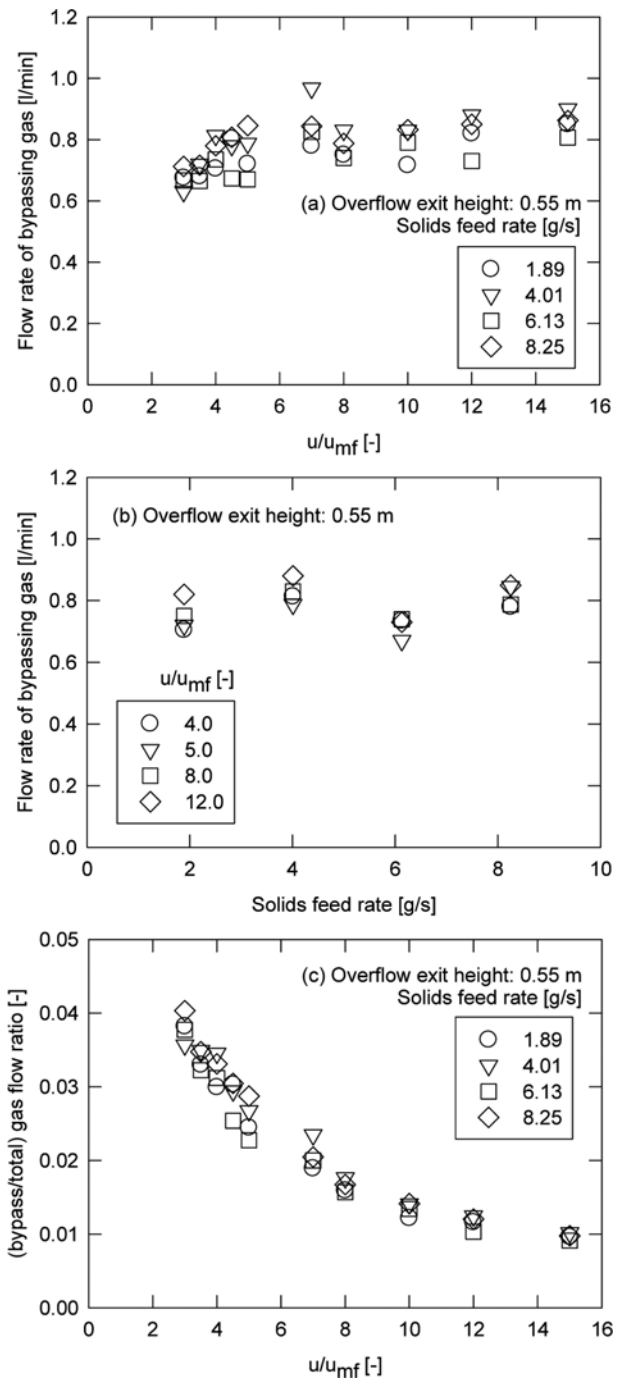


Fig. 5. Flow rate of gas bypassing through the standpipe (height of overflow exit for fluidized solids: 0.55 m): effects of (a), (c) u/u_{mf} and (b) solids feed rate.

ized bed as the fluidizing velocity increased while the solids flow rate was held constant. As the fluidization velocity increased, the bypass gas increased at the ratio of the gas velocity to the minimum fluidizing velocity (u/u_{mf}) less than 5, and almost levelled off at u/u_{mf} greater than 5 (0.7-0.9 l/min; 1.17×10^{-5} - 1.50×10^{-5} m³/s; vertical superficial velocity based on cross section: 0.00515-0.00662 m/s). Gas bubbles were also observed rising up along the upper portion of the standpipe in cross section [4,7]. Fig. 5(b) shows the

change in the flow rate of bypassing gas with increasing solids feed rate when the fluidizing velocity was held constant. The flow rate of bypassing gas remained almost constant, and the effect of the solids feed rate could be neglected. On the basis of the standpipe cross section, the vertical velocity of descending solids ranged from 0.000834 m/s to 0.00364 m/s (see Table 1) and the relative velocity of gas to solids from 0.00598 m/s to 0.0102 m/s, less than the minimum fluidization velocity (0.0125 m/s) of solids. It was believed that the solids were in the fixed bed state or partially in the minimum fluidized state when bubbles appeared.

The pressure loss of the gas due to friction at the walls of the fluidized bed and the standpipe could be almost neglected, and then the pressure loss in both channels of the fluidized bed and the standpipe was mainly due to friction in the solids bed. The pressure drop in both channels, i.e., the driving force of the fluid flow, was the same, and the gas flow rate of each channel was determined to a value satisfying this pressure drop by equilibrium among both gas flow rates and the pressure drop. When the gas velocity increased in the fluidized bed, the pressure drop across the fluidized bed decreased (Fig. 3(a)). At the same time, the solids bed height in the standpipe decreased (Fig. 4(a)), but the descending velocity of solids increased. However, the flow rate of the bypassing gas did not increase continuously in proportion to the fluidizing gas velocity, but stopped its increasing trend (Fig. 5(a)). As a result, at the ratio of u/u_{mf} greater than 5, it was inferred that the flow rate of the bypassing gas was kept constant because the increase in the solids flow rate suppressed the gas flow rising in the standpipe [1]. However, the ratio of the bypass gas to the total gas in flow rate decreased consistently as the fluidization velocity increased (Fig. 5(c)).

The effect of overflow-exit's height of fluidized solids was investigated while the solids feed rate was set at 4.01×10^{-3} kg/s. Fig. 6 shows the pressure drop across the fluidized bed obtained by varying the exit height at various gas velocities. As expected, the pressure drop across the bed increased with the exit height. This was because the increase in the height to which the solids should be carried over by bubbles increased the residence time and then the

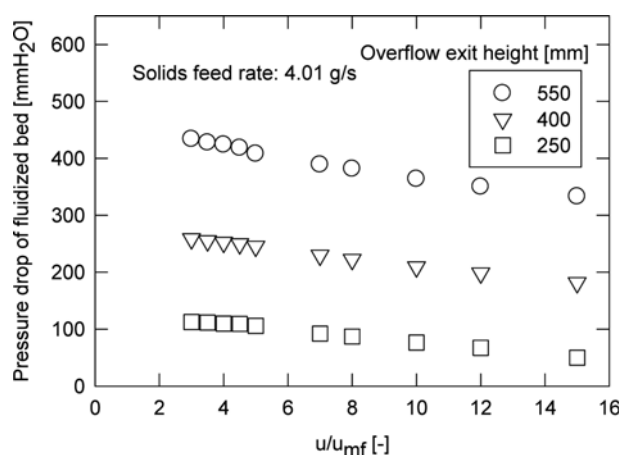


Fig. 6. Effects of u/u_{mf} and height of overflow exit for fluidized solids on pressure drop of the bubbling bed (solids flow rate: 4.01×10^{-3} kg/s).

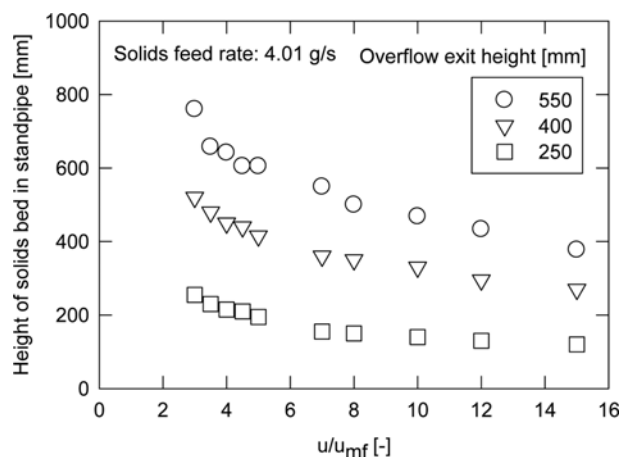


Fig. 7. Effects of u/u_{mf} and height of overflow exit for fluidized solids on height of solids bed in the standpipe (solids flow rate: 4.01×10^{-3} kg/s).

amount of solids in the fluidized bed.

Fig. 7 shows the height of the solids bed within the standpipe obtained by varying the height of overflow exit at various gas velocities. As the exit height increased, the height of the solids bed in the standpipe also increased. This was because the bed pressure drop increasing with the exit height (Fig. 6) enhanced the resistance to the solids entering the fluidized bed. In order for the solids, their own bed height in the standpipe producing the potential head to push themselves into the fluidized bed should be increasing (Fig. 4).

Fig. 8 shows the flow rate of bypassing gas obtained by varying the exit height of fluidized solids while the fluidizing gas velocity was held constant. The effect of the exit height on the flow rate of the bypassing gas appeared small. As the exit height increased, the height of the solids bed in the standpipe also increased proportionally (Fig. 7). As a result, the resistance to the flow of bypassing gas increased, so the change in its flow rate was insignificant.

Based on the experimental results, the correlations on pressure

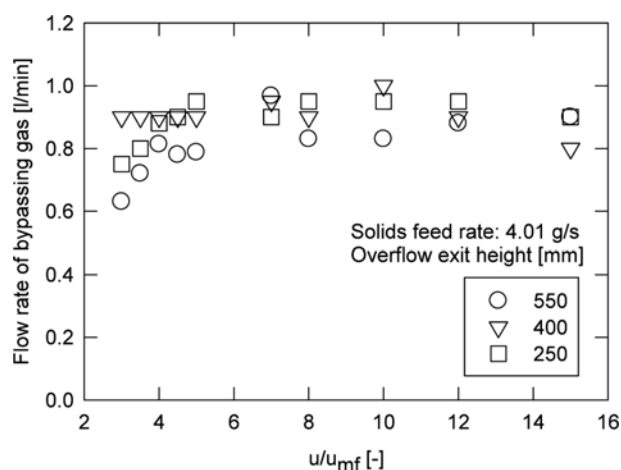


Fig. 8. Effects of u/u_{mf} and exit height of fluidized solids on flow rate of gas bypassing through standpipe (solids feed rate: 4.01×10^{-3} kg/s).

drop across the fluidized bed, height of solids bed in the standpipe, and flow rate of gas bypassing the standpipe were obtained as follows.

$$\Delta p_{bed} = 7681 h_d^{1.755} G_{s,bed}^{0.03089} q_b^{-0.1151}, \quad r^2 = 0.9941 \quad (1)$$

$$h_{st} = 0.5105 h_d^{1.344} G_{s,bed}^{0.03589} q_b^{-0.2795}, \quad r^2 = 0.9861 \quad (2)$$

$$y_g = 0.09036 h_d^{-0.2128} G_{s,sp}^{0.01642} y_e^{2.263}, \quad r^2 = 0.9532 \quad (3)$$

In Eqs. (1) to (3), Δp_{bed} is pressure drop of the fluidized bed [Pa], h_d overflow-exit height of fluidized solids [m], $G_{s,bed}$ solids flux based on area of the fluidized bed [$\text{kg}/\text{m}^2\text{s}$], q_b volumetric bubble flux based on total gas flow rate and the area of the fluidized bed

[m/s], h_{st} static bed height of solids in the standpipe [m], y_g ratio of bypass gas to the total gas in flow rate [-], $G_{s,sp}$ vertical solids flux in the standpipe [$\text{kg}/\text{m}^2\text{s}$], and y_e fraction of gas flowing in the emulsion phase of fluidized bed [-]. The q_b and y_e were written as the following relations [16].

$$q_b = u - u^{0.62} u_{mf}^{0.38} \quad (4)$$

$$y_e = \left(\frac{u_{mf}}{u} \right)^{0.38} \quad (5)$$

Eq. (3) indicates that the flow rate of bypassing gas is dominated by the flow rate of emulsion gas in the fluidized bed.

Gravity is the main driving force that causes the solids in the standpipe to flow down. When the height of the solids bed is the same, the inclined standpipe is smaller in vertical component of gravity acting on the solids bed in the standpipe than in the vertical one. However, this study was carried out on small-scale equipment for the purpose of basic research on the experimental results to investigate the influence of operating variables other than the specification of the equipment, such as column diameter, standpipe diameter and angle of the standpipe. Thus, Eqs. (1) to (3) are applicable for the same size and geometry of the equipment in following ranges: $0.0375 < u [\text{m}/\text{s}] < 0.188$, $0.14 < G_{s,bed} [\text{kg}/\text{m}^2\text{s}] < 1.05$, $0.834 < G_{s,sp} [\text{kg}/\text{m}^2\text{s}] < 3.69$, $0.25 < h_d [\text{m}] < 0.55$. Further studies are needed to investigate the effects of various equipment specifications.

Fig. 9 shows the comparison of the values predicted by correlations with the values measured in experiment. As shown in the figure where the average relative deviations (ARDs) defined by Eq. (4) are denoted, the correlations were in good agreement with the measured data.

$$ARD = \frac{\sum_i^N \left(\frac{Y_{mea} - Y_{cal}}{Y_{mea}} \right)_i}{N} \quad (6)$$

In Eq. (6), N is the number of data, i the data number, Y_{mea} the measured value, and Y_{cal} the value calculated by the correlation.

CONCLUSIONS

Both the pressure drop of the fluidized bed and the height of the solids bed in the standpipe decreased with the fluidizing gas velocity. The flow rate of gas bypassing through the standpipe increased with the fluidizing gas velocity that was less than $5u_{mf}$; however, it levelled off at the fluidizing velocity greater than $5u_{mf}$. Both the pressure drop of the fluidized bed and the height of the solids bed in the standpipe increased with the solids feed rate, of which effect was smaller than that of the fluidizing velocity. The ratio of bypass to total gas in flow rate decreased exponentially with the total gas flow rate. The effect of the solids feed rate on the flow rate of gas bypassing through the standpipe could be ignored. The pressure drop of the fluidized bed and the height of the solids bed in the standpipe increased with the height of the overflow exit for fluidized solids. However, the effect of the height of the overflow exit on the flow rate of gas bypassing through the standpipe was negligible. Correlations on the pressure drop of the fluidized bed, the height of solids bed in the standpipe, and the flow rate

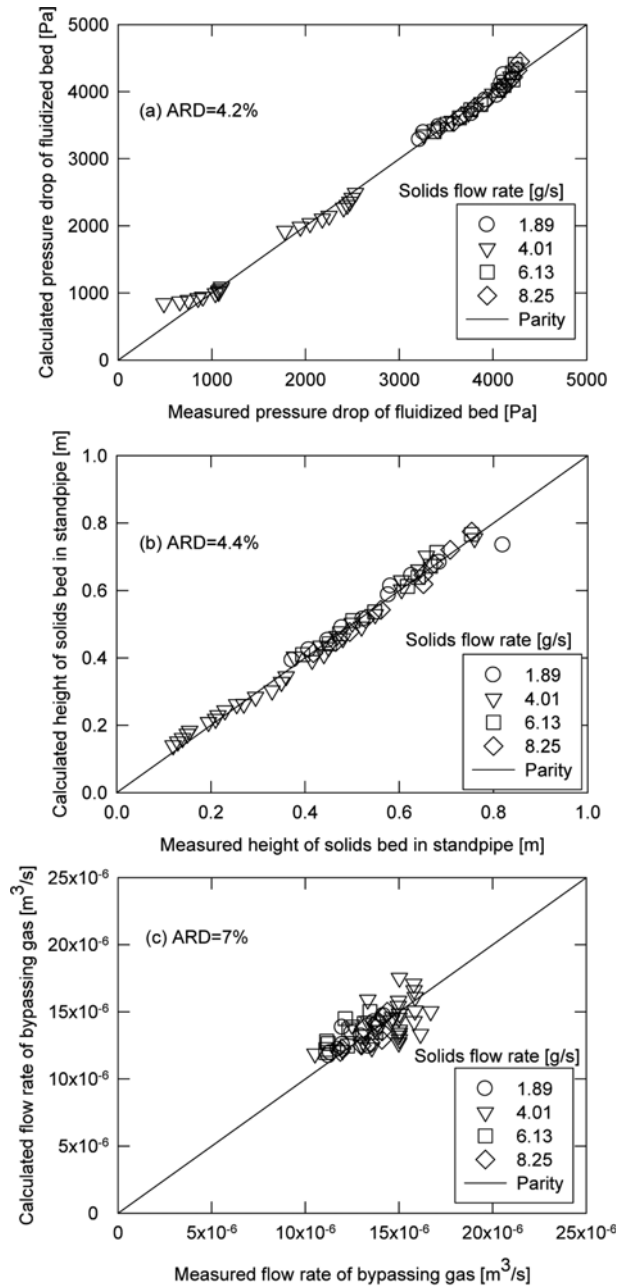


Fig. 9. Comparison between measured data and values calculated by correlations.

of gas bypassing through the standpipe were proposed successfully.

ACKNOWLEDGEMENTS

This work was supported by the Energy Efficiency & Resources of the Korea Institute of Energy Technology Evaluation and Planning (KETEP) grant funded by the Korea government Ministry of Knowledge Economy (20142010201830).

NOMENCLATURE

- d_p : particle diameter or specific surface mean diameter [m]
 $G_{s,bed}$: solids flux based on area of the fluidized bed [$\text{kg}/\text{m}^2\text{s}$]
 $G_{s,sp}$: vertical solids flux in the standpipe [$\text{kg}/\text{m}^2\text{s}$]
 h_{it} : overflow-exit height of fluidized solids [m]
 h_{st} : static bed height of solids in the standpipe [m]
 N : number of data [-]
 ΔP_{bed} : pressure drop of the fluidized bed [Pa]
 q_b : volumetric bubble flux based on total gas flow rate and the area of the fluidized bed [m/s]
 u : fluidizing gas velocity based on total gas flow rate [m/s]
 u_{mf} : minimum fluidizing gas velocity of solids [m/s]
 Y : value [Pa, m, m^3/s]
 Y_e : fraction of gas flowing in the emulsion phase of fluidized bed [-]
 Y_g : ratio of bypass gas to the total gas in flow rate [-]

Subscripts

- cal : calculated [-]
 i : data number [-]
 mea : measured [-]

REFERENCES

1. T.M. Knowlton, in *Circulating Fluidized Beds*, J.R. Grace, A.A. Avidan and T.M. Knowlton Eds., Blackie Academic & Professional, London, UK, 214 (1997).
2. J.H. Choi, C.K. Yi and S.H. Jo, *Korean J. Chem. Eng.*, **28**, 1144 (2011).
3. C.-K. Yi, S.-H. Jo and Y. Seo, *J. Chem. Eng. Japan*, **41**, 691 (2008).
4. R.A. Sauer, I.H. Chan and T.M. Knowlton, *AIChE Symp. Ser.*, **234**, 1 (1984).
5. D.P. O'Dea, V. Rudolph and Y.O. Chong, *Powder Technol.*, **62**, 291 (1990).
6. T. Takeshita, K. Atumi and S. Uchida, *Powder Technol.*, **71**, 65 (1992).
7. S.B.R. Karri and T.M. Knowlton, in *Circulating Fluidized Bed Technology IV*, A. Avidan Ed., AIChE, New York, U.S.A., 253 (1993).
8. A.D. Yaslik, in *Circulating Fluidized Bed Technology IV*, A. Avidan Eds., AIChE, New York, U.S.A., 484 (1993).
9. S.B.R. Karri, T.M. Knowlton and J. Litchfield, in *Fluidization VIII*, J.F. Large and C. Laguerie Eds., Engineering Foundation, New York, U.S.A., 557 (1995).
10. S. Jing, Q. Hu, J. Wang and Y. Jin, *Chem. Eng. Processing: Process Intensification*, **42**, 337 (2003).
11. L. Martin and J.R. van Ommen, *Chem. Eng. J.*, **204-206**, 125 (2012).
12. P.-S. Youn and J.-H. Choi, *Korean Chem. Eng. Res.*, **52**, 81 (2014).
13. D. Kunii and O. Levenspiel, *Fluidization engineering*, 2nd Ed., Butterworth-Heinemann, Boston, U.S.A. (1991).
14. W.L. McCabe, J.C. Smith and P. Harriott, *Unit operations of chemical engineering*, 7th Ed., McGraw-Hill, New York, U.S.A., 98 (2005).
15. P.N. Rowe and B.A. Partridge, in *Proc. Symp. on Interaction between Fluids and Particles*, Inst. Chem. Eng. London, UK, 135 (1962).
16. J.H. Choi, J.E. Son and S.D. Kim, *IEC Research*, **37**, 2559 (1998).